Article

Application of BiVO$_4$/TiO$_2$/CNT Composite Photocatalysts for Membrane Fouling Control and Photocatalytic Membrane Regeneration during Dairy Wastewater Treatment

Elias Jigar Sisay [1,2], Szabolcs Kertész [2], Ákos Fazekas [2], Zoltán Jákói [2], Endre Zsolt Kedves [2], Tamás Gyulavári [3], Áron Ágoston [4], Gábor Veréb [2] and Zsuzsanna László [2,*]

[1] Doctoral School of Environmental Sciences, University of Szeged, Rerrich Béla Sqr. 1, 6720 Szeged, Hungary
[2] Department of Biosystems Engineering, Faculty of Engineering, University of Szeged, Moszkvai Blvd. 9, 6725 Szeged, Hungary
[3] Department of Applied and Environmental Chemistry, Institute of Chemistry, University of Szeged, Rerrich Béla Sqr. 1, 6720 Szeged, Hungary
[4] Department of Physical Chemistry and Materials Science, University of Szeged, Rerrich Béla Sqr. 1, 6720 Szeged, Hungary
[*] Correspondence: zsizsu@mk.u-szeged.hu; Tel.: +36-62-546-525

Abstract: This study aimed to investigate the performance of composite photocatalytic membranes fabricated by incorporating multiple nanoparticles (TiO$_2$, carbon nanotubes, BiVO$_4$) into polyvinylidene fluoride membrane material for real dairy wastewater treatment. The composite photocatalytic membranes exhibited superior antifouling behavior, lower filtration resistance, better flux, and higher flux recovery ratio than the pristine membrane. Salinity, pH, and lactose concentration are determinant factors that affect filtration resistance and rejection performance during the ultrafiltration of dairy wastewater. Generally, higher irreversible and total resistances and slightly lower chemical oxygen demand (COD) rejections were found at higher salinity (expressed by electric conductivity values of >4 mS/cm) than lower salinity (<4 mS/cm) levels. The presence of lactose in dairy wastewater increased irreversible resistance and severely reduced COD rejection during ultrafiltration due to the ability of lactose to pass through the membranes. It was ascertained that membranes require further treatment after filtrating such wastewater. Lower resistances and slightly better COD rejections were observed at pH 7.5 and pH 9.5 compared to those observed at pH 4. Photocatalytic membranes fouled during the ultrafiltration of real dairy wastewater were regenerated by visible light irradiation. The membrane containing all constituents (i.e., TiO$_2$, carbon nanotubes, and BiVO$_4$) showed the best regeneration performance, exceeding that of the pristine membrane by 30%.

Keywords: photocatalytic membranes; antifouling; PVDF; bismuth vanadate; carbon nanotubes; visible light

1. Introduction

The dairy industry generates huge amounts of highly polluted wastewater globally. Generally, it produces 1–10 L of effluent for every liter of milk processed. The effluent contains numerous organic components (such as lactose, casein, fat, and whey protein), inorganic salts, and nitrogenous compounds. In addition, dairy wastewater also contains large amounts of detergents and sanitizers used for washing and a considerable amount of nutrients. These wastewaters can be characterized by high biochemical oxygen demand (BOD) and chemical oxygen demand (COD) [1,2].

The discharge of untreated or partially treated dairy wastewater results in serious environmental problems. For example, eutrophication, occurring as a result of high nutrient content, promotes the growth of algae and bacteria, which depletes oxygen in the aquatic environment. This can result in the gradual loss of aquatic life. Hence, it is essential to treat

such effluents before they are discharged into water bodies. Dairy wastewater is generally treated by physico-chemical and biological methods [1–3]. However, these methods have their drawbacks, including high costs, the need to use chemicals, inefficient removal of pollutants, high energy requirement, and various operational difficulties [1,3].

Recently, membrane technologies have become increasingly prominent in wastewater remediation, offering numerous benefits such as the efficient removal of pollutants, environmental friendliness, cost efficiency, clean and easy operation, flexibility during system design, and compact equipments [4]. Among membrane processes, ultrafiltration (UF) is widely used for the dairy industry due to its good price and performance [1]. Polyvinylidene fluoride (PVDF) is widely used as a membrane material because of its high mechanical strength, thermal stability, and chemical resistance [5,6]. It is soluble in organic solvents and can be used to fabricate porous membranes [7].

Membrane fouling restricts the application of membranes by increasing operating costs and decreasing their lifetime [1]. Many strategies have been developed to prevent fouling, such as optimizing operational conditions [8], functionalization with polymers [9,10], and incorporating nanoparticles [11] and catalysts [8,12–16]. Recently, several catalytic polymeric membranes have been reported as possessing antifouling [12,13] and self-cleaning properties [12,17] and the ability to degrade pollutants [17,18]. Such benefits can be realized by combining filtration and advanced oxidation processes (AOP). During the latter, reactive oxygen species are generated, such as hydroxyl radicals (•OH), to degrade organic pollutants into inorganic molecules. These species can be generated through Fenton-type processes or photocatalysis. Fenton processes include the catalytic decomposition of an oxidant such as hydrogen peroxide (H_2O_2) by a ferrous (Fe^{2+}) or ferric (Fe^{3+}) salt in an acidic medium (pH~3) to form •OH radicals without the application of external energy [19]. Photocatalysis is a process of generating •OH radicals and other reactive oxygen species utilizing light energy and semiconductors such as ZnO, TiO_2, WO_3, V_2O_5, ZrO_2, or Fe_2O_3 [19]. Photocatalysis has been widely studied for membrane cleaning to avoid the excessive use of chemicals and harness the environmentally friendly solar energy [13].

Nowadays, TiO_2-based photocatalytic membranes are widely developed and investigated [13]. However, the relatively high e^-/h^+ recombination rate and low light-utilization rate of TiO_2 restricts their practical application. Numerous attempts have been made to dope TiO_2-based semiconductors to address the problems described above. These attempts include doping with various metals such as Ag [20,21], Au, Pt [20], and zirconia (ZrO_2) [12], as well as non-metals such as graphene [22] and GO [1]. Carbon nanotubes (CNTs) have also received considerable attention due to their outstanding properties, such as high stiffness, flexibility, thermal and electrical conductivities, and large specific surface area. They are broadly used as electron acceptors to reduce the recombination rate of photogenerated charge carriers [23,24]. As TiO_2 has a relatively wide band gap of ~3.15 eV, it can only be efficiently activated under UV light ($\lambda < 390$ nm), while visible light is not utilized [25,26]. To overcome this problem, TiO_2 can be combined with semiconductors having narrower band gaps (such as $BiVO_4$) [27,28], resulting in efficient visible light absorption. Another plausible strategy is to modify TiO_2-containing photocatalysts with good electron acceptors such as CNTs, which may result in more effective visible light activation [29].

In this work, PVDF-based UF membranes were modified with TiO_2, CNT, and $BiVO_4$ nanoparticles according to our previous work [29] via the phase inversion method and applied for synthetic and real dairy wastewater treatment.

2. Results

2.1. Zeta Potential of Prepared Membranes

Zeta potential analysis was performed based on the linear dependence between the streaming potential and pressure gradient. Zeta potentials were calculated using Equation (1). Figure 1a–c illustrates the zeta potentials of unused membranes as a function of pH. The zeta potentials of all membranes are negative at neutral pH. Both modified membranes (Figure 1b,c) had more negative charges than the pristine membrane. This

result is significant considering the pH of dairy wastewater, which is within the range of 7.2–8.8 [30,31]. At these operating pHs, membranes repel negatively charged feed constituents more strongly than the pristine membranes; thus, milk proteins (with an isoelectric point around pH 4.7) are negatively charged in this pH range. This has a considerable contribution to reducing the fouling of membranes.
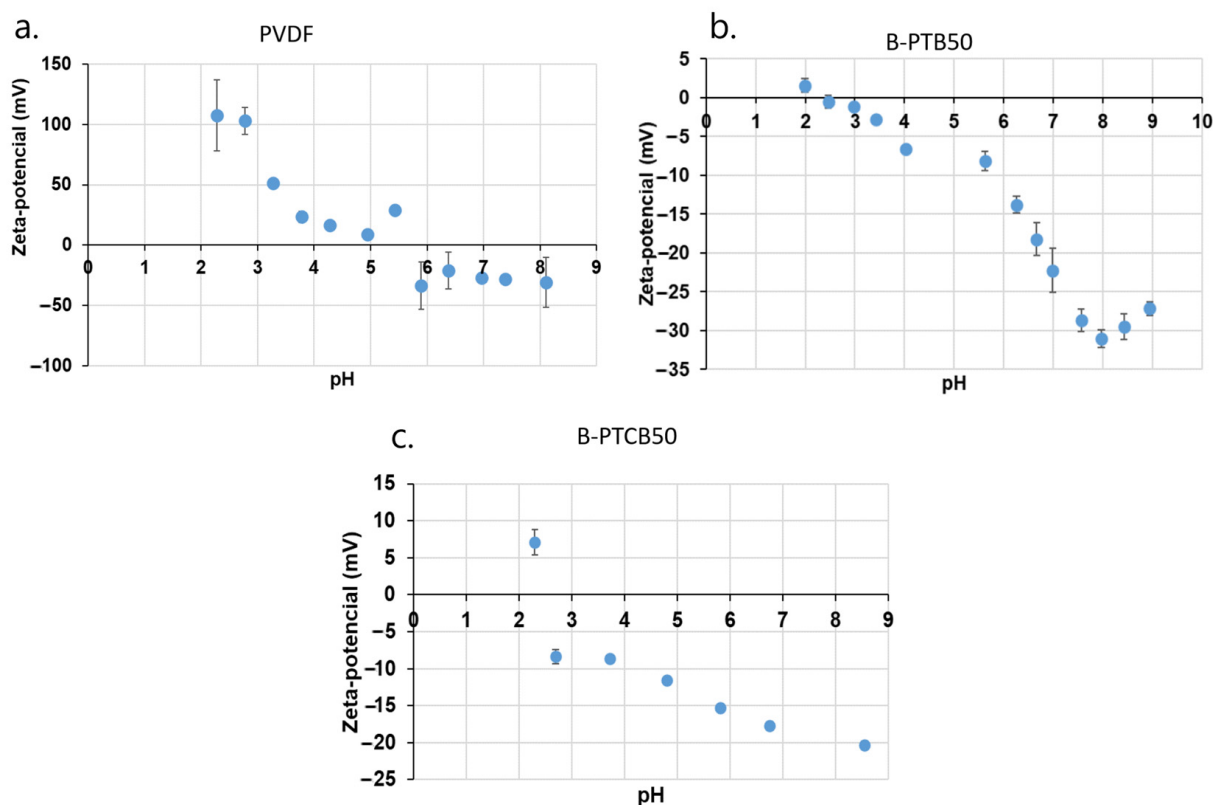

Figure 1. Zeta potentials of unused PVDF, blended PVDF-TiO$_2$/BiVO$_4$ (50–50%) composite (PTB50), and blended PVDF-TiO$_2$/CNT/BiVO$_4$ (48–2–50%) composite (PTCB50) membranes.

2.2. Application of PTCB Membranes for Synthetic Dairy Wastewater Treatment

The experiment aimed to investigate the effect of pH, salinity, and lactose content on the filtration performance of PVDF-, B-PTB50-, and B-PTCB50-blended membranes during the filtration of Bovine serum albumin (BSA) containing synthetic dairy wastewater (SW-BSA).

2.2.1. Effects of Salinity on Fouling and Retention

The effect of salinity on membrane fouling and rejection is shown in Figure 2. The irreversible and total resistances of the modified membranes (B-PTB50 and B-PTCB50) at all salinity levels were lower than those of the pristine PVDF membrane (Figure 2a). This is important from a fouling mitigation perspective. The COD and turbidity rejections of pristine PVDF, B-PTB50, and B-PTCB50 membranes were above 91% at all salinity levels (Figure 2b); however, these membranes show slightly lower COD rejection at the highest salinity level (EC > 4) than at the medium and lowest salinity levels. This could be due to the shielding effect of saline ions. The rejection for turbidity was above 98% for all membranes.
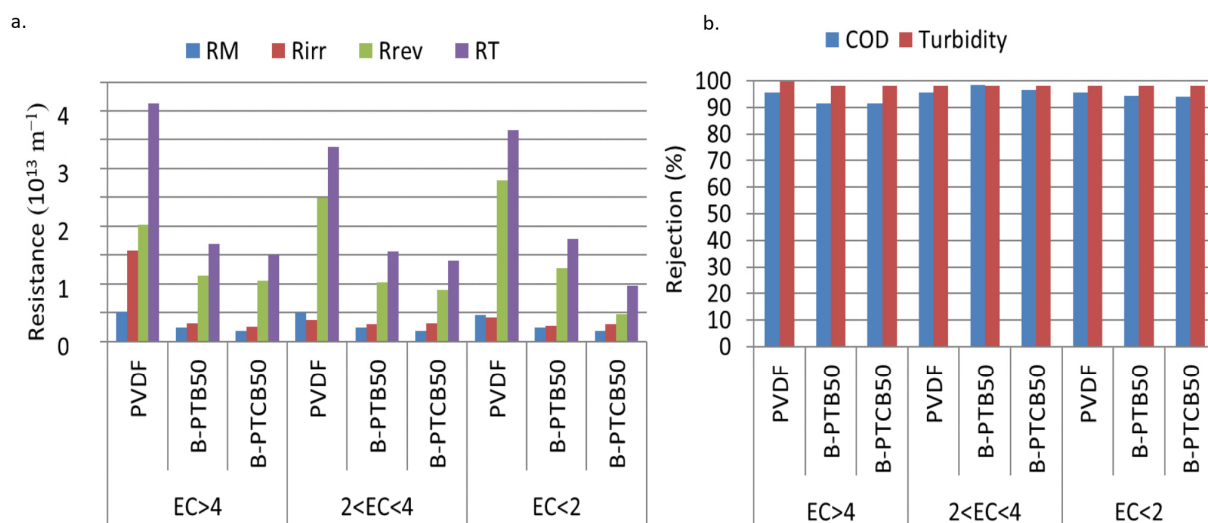
Figure 2. Effect of salinity on membrane fouling during synthetic dairy wastewater membrane filtration expressed by filtration resistances (where *RM* is membrane resistance, *Rirr* is irreversible resistance, *Rrev* is reversible resistance, and *RT* is total resistance) obtained from Equations (Section 3.6.2) (**a**) or COD and turbidity rejections (**b**).

2.2.2. Effects of Lactose on Fouling and Retention

The effects of lactose on membrane fouling and rejection were investigated in the next series of experiments. A lactose level of 0.5 g/L increased the irreversible and total resistances of all membranes, whereas at 1 g/L, the total resistances decreased (Figure 3a). As expected, when the synthetic dairy wastewater contained 1 g/L lactose, the COD rejection of all membranes was reduced to about 50% (Figure 3b). This is because lactose could easily pass through the membranes during filtration. Moreover, in all cases, modifying the membranes resulted in a better performance; the fouling resistances decreased. This means that the blended membranes had considerable antifouling properties even in the presence of lactose.
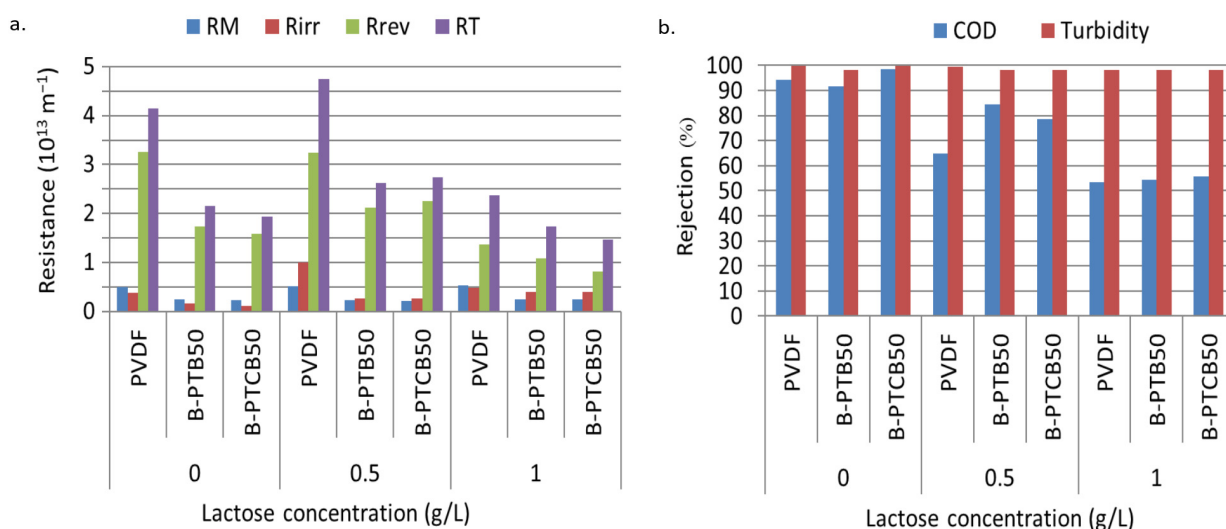

Figure 3. Effect of lactose on membrane fouling during the membrane filtration of BSA and lactose-containing synthetic dairy wastewater (SW-BSA-L) (**a**) and COD and turbidity rejections (**b**).

2.2.3. Effects of pH on Fouling and Rejection

Three different pH values (4, 7.5, and 9.5) were selected to investigate the effect of pH on fouling and rejection (Figure 4). Lower resistances were observed for B-PTB50 and B-PTCB50 at pH 7.5 and pH 9.5, respectively (Figure 4a), compared to the unmodified

PVDF membrane. This is due to the strong repulsion between the negatively charged surface of the membranes and the negatively charged protein (BSA, with an isoelectric point around pH 4.7). At the lower pH (pH 4), higher resistances were observed due to the attraction (van der Waals) forces between the nearly isoelectric membranes (pristine PVDF) and BSA. It is worth noting that irreversible fouling is the parameter that was most efficiently reduced by the membrane modification, which resulted in more negative membrane surfaces. Figure 4b shows the effect of pH on COD and turbidity rejections. It was found that the pH only slightly affected COD rejection, while it did not affect turbidity rejection. Turbidity rejection of all membranes was above 98%, while the COD rejection was above 90%.
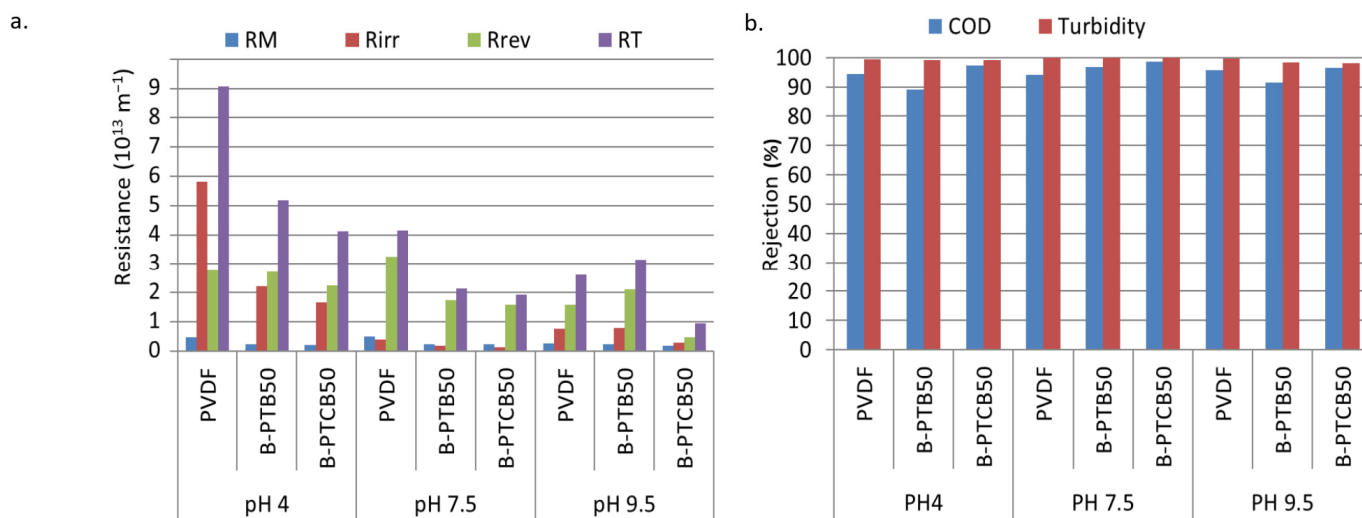

Figure 4. Effect of pH on membrane fouling during the membrane filtration of synthetic dairy wastewater (SW-BSA) (**a**) or COD and turbidity rejections (**b**).

2.3. Application of PTCB Membranes for Real Dairy Wastewater Treatment

This experiment aimed to evaluate the applicability of PVDF-, PTB50-, and PTCB50-blended membranes for real dairy wastewater treatment. The filtration and regeneration performance of PVDF-, B-PTB50-, and B-PTCB50-blended membranes were investigated at pH 7.09.

2.3.1. Filtration Resistances

Filtration resistances of PVDF, B-PTB50, and B-PTCB50 membranes during real dairy wastewater filtration are shown in Figure 5. Higher resistances were observed for unfiltered wastewater (Figure 5a) than for pre-filtered wastewater (Figure 5b). These results indicate the need for pre-filtration during real dairy wastewater treatment by membranes. However, in both cases, the total and irreversible resistances of PVDF membranes were higher than those of the improved (B-PTB50 and B-PTCB50) membranes.

2.3.2. Rejection

The rejection performance of PVDF, B-PTB50, and B-PTCB50 membranes during real dairy wastewater filtration is shown in Figure 6. During the UF of unfiltered and pre-filtered real dairy wastewater, the highest and the lowest COD rejections were 60% and 30% for B-PTCB50 (Figure 6a) and pristine PVDF (Figure 6b), respectively. Almost 100% turbidity rejection was observed in all membranes for unfiltered real dairy wastewater (Figure 6a). The lower rejection performances of the membranes were due to the ability of lactose to pass through the membranes (Figure 6b) which require further treatment.
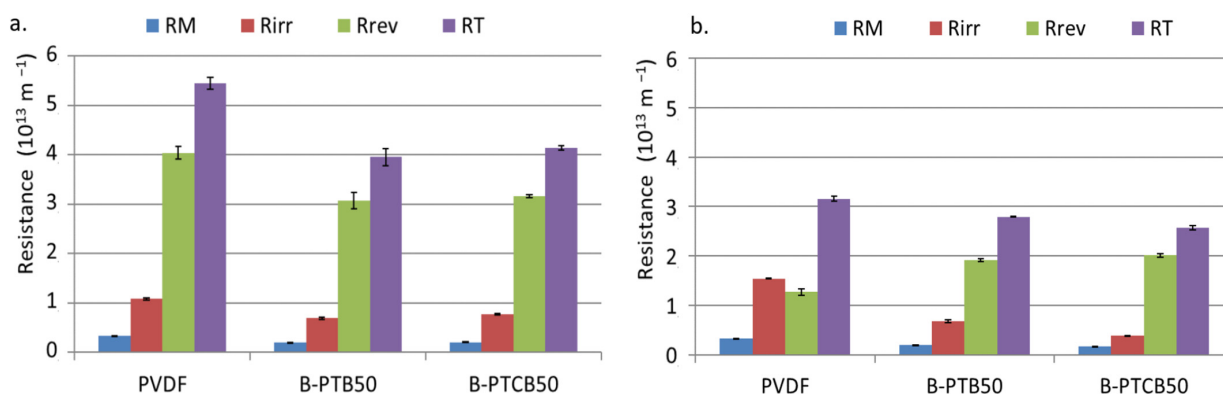
Figure 5. Filtration resistances of PVDF, PTB50, and PTCB50 membranes for real dairy wastewater, using unfiltered (**a**) or pre-filtered (0.2 μm filter paper) wastewater (**b**).
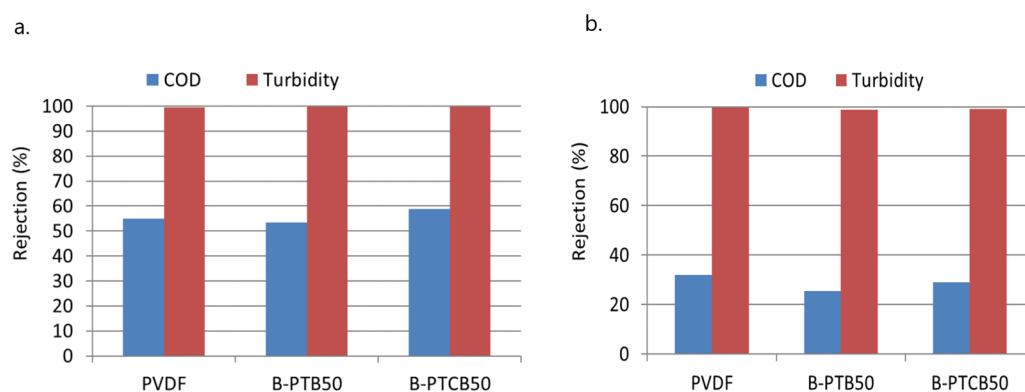

Figure 6. Rejection performance of pristine PVDF, PTB50, and PTCB50 membranes during real dairy wastewater filtration, using unfiltered (**a**) or pre-filtered (0.2 μm filter paper) wastewater (**b**).

2.3.3. Membrane Regeneration

The results of the regeneration of fouled PVDF, B-PTB50, and B-PTCB50 membranes during real dairy wastewater filtration are shown in Figure 7. The regeneration that could be obtained for the modified membranes under 3 h of visible light exposure during the filtration of pre-filtered real dairy wastewater (Figure 7b) was twice/half of what could be achieved during the filtration of unfiltered real dairy wastewater (Figure 7a). Fouled CNT/BiVO$_4$-containing membranes exhibited a better flux restoration after flushing with water than BiVO$_4$-containing membranes (Figure 7b). Moreover, the incorporation of 2% CNTs resulted in a slightly better regeneration performance, probably due to their ability to suppress electron recombination (Figure 7b).
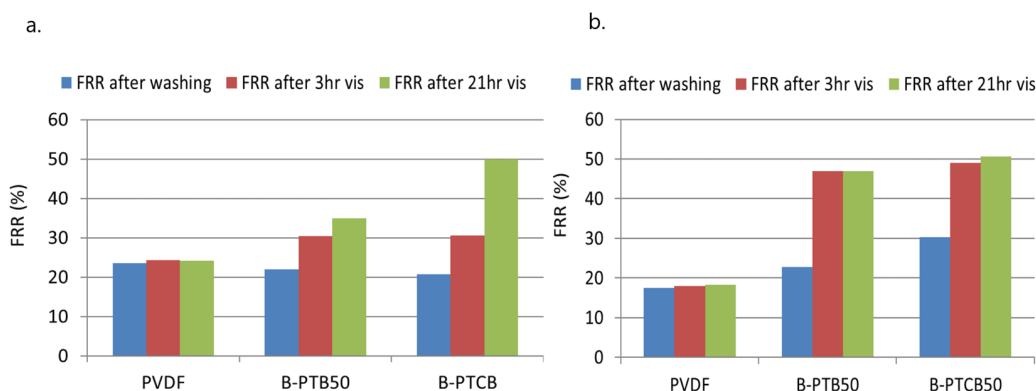

Figure 7. Regeneration performance of fouled PVDF, PTB50, and PTCB50 membranes during real dairy wastewater filtration, using unfiltered (**a**) or pre-filtered (0.2 μm filter paper) wastewater (**b**).

3. Materials and Methods

3.1. Wastewater Collection and Preparation

Membrane filtration experiments were carried out using synthetic and real dairy wastewater. The synthetic dairy wastewater was prepared in our laboratory, while the real dairy wastewater was collected from a nearby milk-processing business.

3.2. Synthetic Dairy Wastewater

Synthetic dairy wastewater was prepared according to the publication of Muniz et al. [3]. It contained bovine serum albumin (BSA) (VWR International KFt, Debrecen, Hungary) and other chemical compounds (synthetic waste, SW) and was labeled as SW-BSA (Table 1) (purchased from VWR International, Debrecen, Hungary).Various concentrations of lactose were added (0, 0.5, and 1 g/L) to the synthetic dairy wastewater to investigate their effect. The SW-BSA samples containing lactose were labeled as SW-BSA-L. The effect of pH on the filtration performance of membranes was investigated by adjusting the pH of the synthetic dairy wastewater with sulfuric acid (1 M) and Na_2HPO_4 (0.1 M).

Table 1. Composition of synthetic dairy wastewater (SW-BSA).

Number	Chemicals	Concentration in g/L
1	BSA	1
2	Ammonium chloride (NH_4Cl)	0.5833
3	Sodium dihydrogen phosphate (NaH_2PO_4)	0.9
4	Sodium bicarbonate ($NaHCO_3$)	1.560
5	Magnesium sulfate heptahydrate ($MgSO_4 \times H_2O$)	0.6
6	Ferrous sulfate heptahydrate ($Fe(SO_4) \times 7H_2O$)	0.024
7	Manganese sulfate monohydrate ($MnSO_4 \times H_2O$)	0.024
8	Calcium chloride ($CaCl_2$ without water)	0.036

The characteristics of synthetic dairy wastewater without lactose and with lactose are presented in Tables 2 and 3, respectively. The absorbance of the model protein solution was measured at a wavelength of 280 nm with a UV–visible spectrophotometer (Hitachi Co., U-2000, Chiyoda City, Japan). EC (electrical conductivity), salinity, and total dissolved solids (TDS) were analyzed with a multi-parameter analyzer (Consort BVBA, Turnhout, Belgium). Turbidity and pH values were measured with a nephelometer (Hach 2100N) and a pH meter (Consort), respectively. Chemical oxygen demand (COD) was analyzed by the potassium dichromate oxidation method. For this purpose, 2 mL of samples was added to test tubes (0–1500 mg/L; (Merck KGaA, Darmstadt, Germany)) and digested at 150 °C for 2 h in a digester (Lovibond ET108; Tintometer, Dortmund, Germany). Last, the values were obtained using a COD photometer (Lovibond PC-CheckIt; Tintometer, Germany).

Table 2. Characteristics of synthetic dairy wastewater (SW-BSA) with various salinity levels.

Level of Salinity	COD	Turbidity	EC (mS)	SAL	TDS (g/L)	pH
High salinity (EC > 4)	1154	46.67	4.14	2.2	2.165	7.5
Medium salinity (2 < EC < 4)	1148	21.83	2.33	1.1	1.25	7.5
Low salinity (EC < 2)	1155	8.16	1.59	0.8	0.85	7.5

Table 3. Characteristics of SW-BSA and SW-BSA-L.

Level of Lactose (g/L)	COD	Turbidity	EC (mS)	SAL	TDS (g/L)	pH
0	1154	46.67	4.14	2.2	2.165	7.5
0.5	1653	158.67	3.83	2.1	2.07	7.88
1	2316	188.33	3.80	2.1	2.23	7.81

3.3. Real Dairy Wastewater

Real dairy wastewater was collected from a milk-processing business (Sole-Mizo, Szeged, Hungary) and kept at 0 °C. The Ca, $CaCO_3$, NH_4^+, NH_3, total N, total P, and PO_4^{3-} contents were analyzed by spectrophotometry (Spectroquant Nova 60; Merck KGaA, Darmstadt, Germany). Biological oxygen demand (BOD) was analyzed with a Lovibond BOD device (Lovibond Oxidirect; Tintometer, Dortmund, Germany). All parameters were expressed as the average of three measurements. The characteristics of the dairy wastewater are shown in Table 4.

Table 4. Physico-chemical characteristics of real industrial dairy wastewater.

Parameter	Average	SD
pH	7.09	0.02
Color	milky white	
EC (mS)	2.1	0.01
TDS (g/L)	1.11	0.01
BOD (mg/L)	2181	70.71
COD (mg/L)	3770	20.00
Ca (mg/L)	159.67	4.04
CaO (mg/L)	231	1.00
$CaCO_3$ (mg/L)	412.33	2.52
NH_4 (mg/L)	56.87	0.31
NH_4N (mg/L)	44.15	0.39
NH_3 (mg/L)	53.31	0.38
NO_3 (mg/L)	10.05	0.83
NO_2N (mg/L)	2.2	0.20
TOTAL N (mg/L)	74.33	1.15
PO_4^{3-} (mg/L)	1178.33	3.51
PO_4-P (mg/L)	40.43	2.60
P_2P_5 (mg/L)	89.61	1.65
TOTAL P (mg/L)	39.10	1.68

3.4. Membrane Preparation

In this study, the phase-inversion method was used to prepare both pristine and improved UF PVDF membranes [29,32]. The polymer-to-solvent ratio during the preparation of UF PVDF membranes was 17.5% to 82.5%. To prepare photocatalytic membranes, we used a photocatalyst: polymer ratio of 1:99. In the TiO_2-$BiVO_4$-based PVDF membrane (B-PTB50), each photocatalyst accounts for 50% of the total photocatalyst amount in the polymer. When this membrane was further modified with CNTs (B-PTCB50), the amounts of TiO_2, CNT, and $BiVO_4$ used were 48%, 2%, and 50% of the total photocatalyst amount in the polymer, respectively. Before membrane preparation, the nanoparticles and PVDF powder were dried in an oven at 80 °C for 4 h. The dried nanoparticles were dissolved in an N-Methyl-2 pyrrolidone (NMP) solution and ultrasonicated for 1 min. Then, the powder was added to the solution under continuous magnetic stirring at 50 °C for 12 h. Afterward, the solution was kept in the dark without stirring for another 12 h to remove air bubbles. For the same purpose, the casting dope solutions were ultrasonicated for 30 min. Figure 8 shows the scheme of membrane preparation using the phase-inversion method. In this method, the solution poured on the glass plate was cast by a casting blade (400 µm thickness) and kept at rest for 30 s for skin layer formation. Then, the glass plates containing the casted solution were put into a bath containing a 3 g/L surfactant solution (sodium dodecyl sulfate) at 15 °C for 3 h. Last, the system was stored in distilled water overnight.
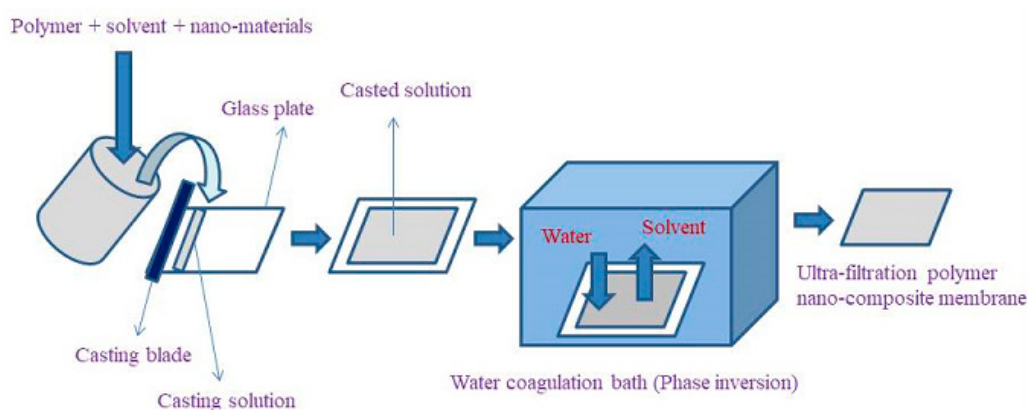
Figure 8. Schematic representation of the phase inversion method.

3.5. Membrane Characterization

Zeta Potential Analysis

Membranes were already characterized in our earlier work (Sisay et al., 2022). Zeta potentials of membranes were calculated using the Helmholtz-Smoluchowski equation (Equation (1)) [33]:

$$\zeta = \frac{\Delta E}{\Delta P} \cdot \frac{\eta}{\varepsilon_{rel}\,\varepsilon_0} \cdot K_B \tag{1}$$

where ζ is the apparent zeta potential; $\Delta E/\Delta P$ is the streaming potential developed as a result of an applied pressure gradient; η and ε_{rel} are the dynamic viscosity and dielectric coefficient of water, respectively; ε_0 is the permittivity of vacuum; K_B is the electric conductivity of the aqueous solution.

3.6. Membrane Filtration Experiments

3.6.1. Water Flux and Contaminant Rejection Performance

The filtration performance of the membranes was evaluated using synthetic or real dairy wastewater. Figure 9 presents a dead-end filtration setup involving a Millipore dead-end cell (Millipore, XFUF04701,Merck KGaA, Darmstadt, Germany). Prior to the filtration experiments (compaction), distilled water was allowed to pass through a 0.0035 m^2 membrane for 30 min. The volume reduction ratio (VRR) of each filtration experiment was fixed to be five, and each experiment was performed at 0.1 MPa and 350 rpm with a built-in magnetic stirrer. The flux and rejection performance of the prepared membranes was calculated based on Equations (2) and (4):

$$J = \frac{W}{A \cdot t} \tag{2}$$

where J refers to the flux (kg/m^2 h); W refers to the weight of permeate (kg); A means the area of effective membrane (m^2); and τ means the time (s).

The VRR was obtained by Equation (3):

$$VRR = \frac{V_0}{V_0 - V_f} \tag{3}$$

where V_0 stands for the initial volume, while V_f stands for the final volume.

The rejection of contaminants was calculated by Equation (4):

$$\text{Rejection }(\%) = \frac{c_1 - c_2}{c_1} \times 100\% \tag{4}$$

where c_1 and c_2 are the concentrations of contaminants in the feed and permeate, respectively.
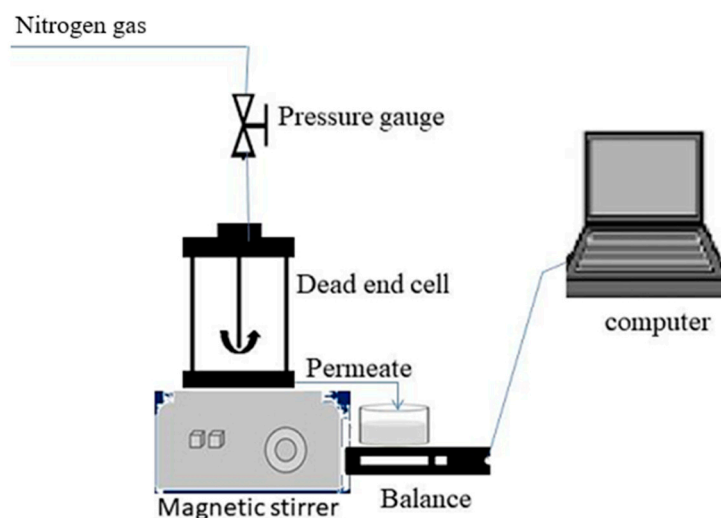
Figure 9. Graphical illustration of the dead-end filtration setup.

3.6.2. Fouling Models

Information about membrane fouling was obtained from filtration resistances which were calculated using the resistances-in-series model [34]. This model estimates individual and overall resistances (Table 5).

Table 5. Formulas for filtration resistances.

Resistances (m^{-1})	Formula
Membrane resistance	$RM = \frac{\Delta P}{J_0 \times \eta w}$
	$Rirrev = \frac{\Delta P}{JW \times \eta w} - RM$
Reversible resistance	$Rrev = \frac{\Delta P}{Jw \times \eta ww} - RF - RM$
Overall resistance	$RT = RM + Rirr + Rrev$

In Equations (Table 5), Δp is the change of pressure (Pa), J_0 is initial water flux (Lm^{-2} h^{-1}), Jw is the flux of the fouled membrane, JW is the water flux after the fouled membrane is rinsed (L/m^2 h), ηW is the viscosity of water (Pas), and ηww is the viscosity of wastewater.

Antifouling performances of the prepared membranes were examined based on the same fouling experiment using the flux recovery ratio (FRR) and obtained by the following equation (Equation (5)):

$$\text{FRR} = \frac{J_c}{J_0} \cdot 100 \tag{5}$$

where J_0 is initial water flux (Lm^{-2} h^{-1}) and Jc is the water flux of the used membrane after cleaning (Lm^{-2} h^{-1}).

Membrane regeneration efficiency was investigated by performing flux recovery experiments in the photocatalytic membrane reactors. For this purpose, the water fluxes of the fouled and flushed (with distilled water) membranes were measured after the filtration of dairy wastewater. The regeneration experiments were performed using the filtration cell as a photoreactor. This cylindric reactor had a diameter of 7.45 cm and was equipped with a 1 m long LED strip (5050 SMD, "cool white," 600 lm/m light intensity). The membrane was placed at the bottom of the cylinder. The fluxes were measured after 3 h and 21 h of visible light exposure.

4. Conclusions

Industrial dairy wastewater treatment using composite photocatalytic PVDF membranes offers promising solutions for many environmental concerns, specifically water scarcity and pollution. These membranes also provide a golden opportunity to use visible light for membrane cleaning, reducing the use of environmentally unfriendly chemicals and costly UV light.

This study aimed to fabricate composite photocatalytic membranes by incorporating multiple nanoparticles (TiO$_2$, CNT, BiVO$_4$) into PVDF membranes and investigate their performance for real dairy wastewater treatment. The membranes were prepared by the phase-inversion method.

The composite photocatalytic membranes exhibited superior antifouling behavior, lower filtration resistance, better flux, and higher FRR than the pristine membrane. Salinity, pH, and lactose concentration are determinant factors that affect filtration resistance and rejection performance. Generally, higher irreversible and total resistances and slightly lower COD rejection were observed at a higher EC level (>4). Irreversible and total resistances of the modified (B-PTB50 and B-PTCB50) membranes at various salinity levels were lower than those of the pristine PVDF membrane, proving that the modification resulted in better fouling-mitigation properties.

The presence of lactose increased the irreversible resistance and severely reduced COD rejection.

Negatively charged membranes showed lower resistances and slightly better COD rejection at pH 7.5 and pH 9.5 as compared to pH 4. The lower resistance at higher pH was due to the strong repulsion between the negatively charged surface of the membranes and the negative charge of the protein.

Both B-PTB50 and B-PTCB50 showed lower total resistance and better membrane cleaning (FRR) properties during the UF of real dairy wastewater than the pristine membrane. However, all the membranes exhibited lower COD rejection due to the ability of lactose to pass through the membranes, which consequently require further treatment.

Fouled TiO$_2$-CNT-BiVO$_4$-PVDF membrane showed the best regeneration performance, improving that of the pristine membrane by 30%.

References

1. Zinadini, S.; Vatanpour, V.; Zinatizadeh, A.A.; Rahimi, M.; Rahimi, Z.; Kian, M. Preparation and characterization of antifouling graphene oxide/polyethersulfone ultrafiltration membrane: Application in MBR for dairy wastewater treatment. *J. Water Process Eng.* **2015**, *7*, 280–294. [CrossRef]
2. Ahmad, T.; Aadil, R.M.; Ahmed, H.; ur Rahman, U.; Soares, B.C.V.; Souza, S.L.Q.; Cruz, A.G. Treatment and utilization of dairy industrial waste: A review. *Trends Food Sci. Technol.* **2019**, *88*, 361–372. [CrossRef]

3.　　Muniz, G.L.; Borges, A.C.; da Silva, T.C.F. Performance of natural coagulants obtained from agro-industrial wastes in dairy wastewater treatment using dissolved air flotation. *J. Water Process Eng.* **2020**, *37*, 101453. [CrossRef]

4.　　Catenacci, A.; Bellucci, M.; Yuan, T.; Malpei, F. Dairy wastewater treatment using composite membranes. In *Current Trends and Future Developments on Bio Membranes*; Elsevier: Amsterdam, The Netherlands, 2020; pp. 261–288. [CrossRef]

5.　　Sobola, D.; Kaspar, P.; Částková, K.; Dallaev, R.; Papež, N.; Sedlák, P.; Trčka, T.; Orudzhev, F.; Kaštyl, J.; Weiser, A.; et al. PVDF Fibers Modification by Nitrate Salts Doping. *Polymers* **2021**, *13*, 2439. [CrossRef]

6.　　Kaspar, P.; Sobola, D.; Částková, K.; Dallaev, R.; Šťastná, E.; Sedlák, P.; Knápek, A.; Trčka, T.; Holcman, V. Case Study of Polyvinylidene Fluoride Doping by Carbon Nanotubes. *Materials* **2021**, *14*, 1428. [CrossRef]

7.　　Ji, J.; Liu, F.; Hashim, N.A.; Abed, M.R.M.; Li, K. Poly(vinylidene fluoride) (PVDF) membranes for fluid separation. *React. Funct. Polym.* **2015**, *86*, 134–153. [CrossRef]

8.　　Fan, G.; Chen, C.; Chen, X.; Li, Z.; Bao, S.; Luo, J.; Yan, Z. Enhancing the antifouling and rejection properties of PVDF membrane by Ag3PO4-GO modification. *Sci. Total Environ.* **2021**, *801*, 149611. [CrossRef]

9.　　Wei, Q.; Wu, C.; Zhang, J.; Cui, Z.; Jiang, T.; Li, J. Fabrication of surface microstructure for the ultrafiltration membrane based on "active–passive" synergistic antifouling and its antifouling mechanism of protein. *React. Funct. Polym.* **2021**, *169*, 105068. [CrossRef]

10.　　Gholami, S.; Llacuna, J.L.; Vatanpour, V.; Dehqan, A.; Paziresh, S.; Cortina, J.L. Impact of a new functionalization of multiwalled carbon nanotubes on antifouling and permeability of PVDF nanocomposite membranes for dye wastewater treatment. *Chemosphere* **2022**, *294*, 133699. [CrossRef]

11.　　Farahani, M.H.D.A.; Vatanpour, V. A comprehensive study on the performance and antifouling enhancement of the PVDF mixed matrix membranes by embedding different nanoparticles: Clay, functionalized carbon nanotube, SiO$_2$ and TiO$_2$. *Sep. Purif. Technol.* **2018**, *197*, 372–381. [CrossRef]

12.　　Coelho, F.E.B.; Deemter, D.; Candelario, V.M.; Boffa, V.; Malato, S.; Magnacca, G. Development of a photocatalytic zirconia-titania ultrafiltration membrane with antifouling and self-cleaning properties. *J. Environ. Chem. Eng.* **2021**, *9*, 106671. [CrossRef]

13.　　Wang, X.; Li, S.; Chen, P.; Li, F.; Hu, X.; Hua, T. Photocatalytic and antifouling properties of TiO$_2$-based photocatalytic membranes. *Mater. Today Chem.* **2022**, *23*, 100650. [CrossRef]

14.　　Yang, Y.; Yang, L.; Yang, F.; Bai, W.; Zhang, X.; Li, H.; Duan, G.; Xu, Y.; Li, Y. A bioinspired antibacterial and photothermal membrane for stable and durable clean water remediation. *Mater. Horiz.* **2023**, *10*, 268–276. [CrossRef] [PubMed]

15.　　Xu, Y.; Hu, J.; Zhang, X.; Yuan, D.; Duan, G.; Li, Y. Robust and multifunctional natural polyphenolic composites for water remediation. *Mater. Horiz.* **2022**, *9*, 2496–2517. [CrossRef]

16.　　Bai, H.; He, P.; Hao, L.; Fan, Z.; Niu, R.; Tang, T.; Gong, J. Waste-treating-waste: Upcycling discarded polyester into metal–organic framework nanorod for synergistic interfacial solar evaporation and sulfate-based advanced oxidation process. *Chem. Eng. J.* **2023**, *456*, 140994. [CrossRef]

17.　　Chen, L.; Yang, B.; Zhou, P.; Xu, T.; He, C.; Xu, Y.; Zhao, W.; Zhao, C. A polyethersulfone composite ultrafiltration membrane with the in-situ generation of CdS nanoparticles for the effective removal of organic pollutants and photocatalytic self-cleaning. *J. Membr. Sci.* **2021**, *638*, 119715. [CrossRef]

18.　　Zhang, H.; Zhang, J.; Luo, J.; Wan, Y. A novel paradigm of photocatalytic cleaning for membrane fouling removal. *J. Membr. Sci.* **2022**, *641*, 119859. [CrossRef]

19.　　Titchou, F.E.; Zazou, H.; Afanga, H.; El Gaayda, J.; Ait Akbour, R.; Nidheesh, P.V.; Hamdani, M. Removal of organic pollutants from wastewater by advanced oxidation processes and its combination with membrane processes. *Chem. Eng. Process. Process. Intensif.* **2021**, *169*, 108631. [CrossRef]

20.　　Nasr, O.; Mohamed, O.; Al-Shirbini, A.-S.; Abdel-Wahab, A.-M. Photocatalytic degradation of acetaminophen over Ag, Au and Pt loaded TiO$_2$ using solar light. *J. Photochem. Photobiol. A Chem.* **2019**, *374*, 185–193. [CrossRef]

21.　　Nair, A.K.; Jagadeesh Babu, P.E. Ag-TiO$_2$ nanosheet embedded photocatalytic membrane for solar water treatment. *J. Environ. Chem. Eng.* **2017**, *5*, 4128–4133. [CrossRef]

22.　　Jiang, M.; Zhang, M.; Wang, L.; Fei, Y.; Wang, S.; Núnez-Delgado, A.; Bokhari, A.; Race, M.; Khataee, A.; Klemes, J.; et al. Photocatalytic degradation of xanthate in flotation plant tailings by TiO$_2$/ graphene nanocomposites. *Chem. Eng. J.* **2022**, *431*, 134104. [CrossRef]

23.　　Trapalis, A.; Todorova, N.; Giannakopoulou, T.; Boukos, N.; Speliotis, T.; Dimotikali, D.; Yu, J. TiO$_2$/graphene composite photocatalysts for NOx removal: A comparison of surfactant-stabilized graphene and reduced graphene oxide. *Appl. Catal. B Environ.* **2016**, *180*, 637–647. [CrossRef]

24.　　Selvaraj, M.; Hai, A.; Banat, F.; Haija, M.A. Application and prospects of carbon nanostructured materials in water treatment: A review. *J. Water Process Eng.* **2020**, *33*, 100996. [CrossRef]

25.　　Akhavan, O. Lasting antibacterial activities of Ag–TiO$_2$/Ag/a-TiO$_2$ nanocomposite thin film photocatalysts under solar light irradiation. *J. Colloid Interface Sci.* **2009**, *336*, 117–124. [CrossRef] [PubMed]

26.　　Zouzelka, R.; Kusumawati, Y.; Remzova, M.; Rathousky, J.; Pauporté, T. Photocatalytic activity of porous multiwalled carbon nanotube-TiO$_2$ composite layers for pollutant degradation. *J. Hazard. Mater.* **2016**, *317*, 52–59. [CrossRef] [PubMed]

27.　　Malathi, A.; Arunachalam, P.; Kirankumar, V.S.; Madhavan, J.; Al-Mayouf, A.M. An efficient visible light driven bismuth ferrite incorporated bismuth oxyiodide (BiFeO$_3$/BiOI) composite photocatalytic material for degradation of pollutants. *Opt. Mater.* **2018**, *84*, 227–235. [CrossRef]

28. Ratova, M.; Redfern, J.; Verran, J.; Kelly, P.J. Highly efficient photocatalytic bismuth oxide coatings and their antimicrobial properties under visible light irradiation. *Appl. Catal. B Environ.* **2018**, *239*, 223–232. [CrossRef]

29. Sisay, E.J.; Veréb, G.; Pap, Z.; Gyulavári, T.; Ágoston, Á.; Kopniczky, J.; Hodúr, C.; Arthanareeswaran, G.; Sivasundari, G.K.; László, Z. Visible-light driven photocatalytic PVDF-TiO$_2$/CNT/BiVO$_4$ hybrid nanocomposite ultrafiltration membrane for dairy wastewater treatment. *Chemosphere* **2022**, *307*, 135589. [CrossRef]

30. Qazi, J.I.; Nadeem, M.; Baig, S.S.; Baig, S.; Syed, Q. Anaerobic fixed-film biotreatment of dairy wastewater. *Middle East J. Sci. Res.* **2011**, *8*, 590–593.

31. Deshannavar, U.B.; Basavaraj, R.K.; Naik, N.M. High-rate digestion of dairy industry effluent by upflow anaerobic fixed-bed reactor. *J. Chem. Pharm. Res.* **2012**, *4*, 2895–2899.

32. Srivastava, H.P.; Arthanareeswaran, G.; Anantharaman, N.; Starov, V.M. Performance of modified poly(vinylidene fluoride) membrane for textile wastewater ultrafiltration. *Desalination* **2011**, *282*, 87–94. [CrossRef]

33. Lawrence, N.D.; Perera, J.M.; Iyer, M.; Hickey, M.W.; Stevens, G.W. The use of streaming potential measurements to study the fouling and cleaning of ultrafiltration membranes. *Sep. Purif. Technol.* **2006**, *48*, 106–112. [CrossRef]

34. Vatanpour, V.; Yekavalangi, M.E.; Safarpour, M. Preparation and characterization of nanocomposite PVDF ultrafiltration membrane embedded with nanoporous SAPO-34 to improve permeability and antifouling performance. *Sep. Purif. Technol.* **2016**, *163*, 300–309. [CrossRef]